Reassessment of the *Alticola roylei* species group in Northern Pakistan through morphology, molecular systematics, and biogeography

Research Thesis
Presented in partial fulfillment of the requirements for graduation with research distinction in the undergraduate colleges of The Ohio State University

by
Shivani Bhatt
The Ohio State University July 2020

Project Advisor: Dr. Ryan W. Norris, Department of Evolution, Ecology, and Organismal Biology

High elevation mountain ranges contribute to the speciation of mammal species. Mountain voles (genus *Alticola*) inhabit high elevations in Central Asia. Within the genus, taxonomic relationships among the *Alticola roylei* species group are primarily determined by morphological characteristics such as the distinctive M^3 molar and tail length. We hypothesized that the mountain ranges of Northern Pakistan inhabited by these species, along with valley and river barriers, may present an opportunity for diversification in this group. I combined molecular data (n=83) and morphological data (n=118) to analyze individuals of the *Alticola roylei* species group. I sequenced individuals using the *Cytb* gene and utilized the sequences to construct a phylogenetic tree under a Bayesian framework. We compared these results to morphological characters including M^3 molar (obtained by collaborator Eve Rowland), and external measurements. We observed the morphological measurements may not be diagnostic in determining the boundaries of the species. Distinct clades seem to occupy specific geographic distributions across Northern Pakistan. Molecular data places individuals together that may vary in diagnostic morphological criteria.

INTRODUCTION

The name *Alticola* derives from Latin roots *altus* meaning "high" and -*cola* meaning "dweller of" (Kryštufek et al. 2017). Mountain voles of the genus *Alticola* inhabit high elevation areas across Central Asia, ranging from 500-4,300 m (Pardiñas et al. 2017). While the value of 500 m may not seem to suggest high elevation, the lower range of values correspond to species found in the northern extent of the geographic scope. According to Roberts (1997), these mountain voles and pikas share similarities in ecology and behavior. Both prefer to inhabit rocky areas and talus slopes, and do not exhibit burrowing behavior occupying cracks instead (Roberts 1997). This type of ecology and behavior distinguish members of *Alticola* from other voles. Like pikas, members of *Alticola* collect vegetable matter that is distributed into heaps for consumption throughout the winter (Roberts 1997). In general, these voles feed on roots, seeds, and green plants (Roberts 1997). However, with invertebrates, flowers, fruits, bark, mosses, and lichens also contributing to their diet (Roberts 1997).

Classification of the *Alticola* genus requires an examination of its complex taxonomic history. The rodent family Cricetidae includes the subfamily Arvicolinae and tribe Myodini (Pardiñas et al. 2017; Tang et al.2018). Arvicolines include voles, lemmings, and muskrats. Tribe Myodini is comprised of 36 species of voles divided into 7 genera: *Alticola*, *Aschizomys, Caryomys*, *Craseomys, Eeothenomys*, *Hyperacrius*, and *Myodes* (Pardiñas et al. 2017; Tang et al.2018). While taxonomic uncertainty persists among these genera, differences emerge to distinguish *Alticola* from other genera. Morphological data gathered by Philips (1969) show that *Hyperacrius*, a genus whose range overlaps with *Alticola*, displays a cranial interorbital ridge, absent in *Alticola*. Occurrence of *Hyperacrius* in forest and meadow habitat as opposed to the rocky habitat of *Alticola* further distinguishes *Hyperacrius* from *Alticola* (Philips 1969).

Phylogenetic reconstruction performed by Tang et al. (2018) begins to resolve the previous taxonomic uncertainty between *Alticola* and its sister genus *Myodes* (including *Craseomys*), through the utilization of multiple nuclear genes rather than a single gene. Furthermore, morphological analysis reveals that *Myodes* exhibits more lingual salient angles as well as an extended posterior lobe in the third molar tooth, when compared to *Alticola* (Tang et al.2018).

The genus *Alticola* includes multiple species of voles that inhabit mountainous or rocky habitats across Central Asia. Until recently, the genus *Alticola* had been divided into three subgenera *Alticola sensu stricto*, *Platycranius*, and *Aschizomys* (Musser and Carleton 2005; Lebedev 2007). Phylogenetic analyses have demonstrated that *Aschizomys* is more closely related to *Myodes* (Kohli et al. 2014; Tang et al. 2018) and is now recognized as a distinct genus (Pardiñas et al. 2017). The subgenus *Platycranius* had been erected for the monotypic *A.* (*Platycranius*) *strelzovi*, but Tang et al. (2018) showed that the subgenus *Alticola* is paraphyletic with respect to *A. strelzovi*. Although no longer divided into subgenera, the 10 species in the genus *Alticola* are split into species groups. Within the subgenus *Alticola s.str*, the *Alticola stoliczkanus* voles are considered a distinct species group due to their morphological characters and geographic range compared to their sister taxon (the *Alticola roylei* species group) (Kryštufek et al.2017). Mountain voles in the *A. stoliczkanus* species group exhibit short, densely clad tails and a third upper molar tooth with fewer lingual salient angles, as well as occupy a geographic range that extends into the Nepal-China border (Kryštufek et al.2017). *Alticola s.str.* also includes the *Alticola roylei* species group which includes the morphologically similar species of *A. montosus, A. albicauda,* and *A. argentatus* (Kryštufek et al.2017).

Morphological traits specific to the *A. roylei* species group include a distinctive third upper molar tooth with three lingual salient angles, a moderately long tail, and an unflattened

skull (Kryštufek et al. 2017). *Alticola montosus* exhibits a pronounced difference in the third upper molar tooth (Table 1) compared to *A. argentatus* and *A. albicauda* due to the isolation of its antero-buccal triangle from the anterior loop (Kryštufek et al. 2017). Similarly, the shorter tail (Table 1) length in proportion to head and body length of *A. albicauda* distinguishes *A. albicauda* from the proportionally moderate tail length of *A. montosus and A. argentatus (*Kryštufek et al. 2017). According to Kryštufek et al. (2017), the range of the *A. roylei* species group remains distinct from the range of the *A. stoliczkanus* species group, as the *A. stoliczkanus* species group inhabits areas west of Nepal. Within the areas inhabited by the *A. roylei* species group, *A. argentatus* encompasses a relatively broad geographic scope (Pardiñas et al. 2017). The Tien Shan, Pamir, Karakorum, and Hindu Kush mountains further divides *A. argentatus* into subspecies *A. a blanfordi* (Gilgit-Baltistan in N Pakistan and NW India), *A. a parvidens* (Khyber Paktunkhwa Province in N Pakistan), *A. a phasma* (E Karakorum in SW China, Xizang), *A. a severtzovi* (Tien Shan Mts in Kazakhstan and Kyrgyzstan), *A. a subluteus* (Tien Shan Mts in E Kazakhstan, Kyrgyzstan and SW China, Xinjian), *A. a tarasovi* (Tien Shan Mts in Kyrgyzstan and NW China, Xinjian), and *A. a worthingtoni* (Basin of Tekes, Tien Shan Mts, Xinjiang, NW China) (Nadachowski and Mead 1999; Pardiñas et al. 2017). Many of these designations are poorly defined. As we are interested in the geographic distribution of voles specific to Northern Pakistan, the restricted distribution of *A. roylei* to the mountain ranges of Northern India are of less interest to us (Kryštufek et al.2017).

Northern Pakistan houses mountains of extremely high elevations, including K2 (world's 2nd highest mountain) and Nanga Parbat (world's 9th highest mountain). Hindu Kush, Karakoram, and Himalayan mountains of Northern Pakistan are characterized by the glaciation that took place in the Late Quaternary Period (Kamp and Owen 2011). Unique climatic

conditions drive the formation of these glaciers; the mid-latitude westerlies and the South Asian monsoon (Kamp and Owen 2011). The mid-latitude westerlies create conditions of relatively higher precipitation in the winter seasons, while the South Asian monsoon creates conditions of relatively higher precipitation in the summer seasons due to the incoming moisture from the Indian Ocean (Kamp and Owen 2011). These underlying seasonal conditions also contribute to the maintenance of the glaciers (Kamp and Owen 2011). Previous researchers examined the moraines left by glacier deposits in order to predict where the glaciers terminated (Kamp and Owen 2011). Moraines examined from the Chitral, Ghizar, and Swat-Kohistan valleys within the Hindu Kush showed a complex ice-stream network with glaciers advancing from the Gilgit Valley into the Indus Valley (Kamp and Owen 2011). Similarly, the glaciated valleys of the Central Karakoram mountains drain into the Indus Valley (Kamp and Owen 2011). Nanga Parbat valley in the Himalayan mountains may be the last area where glaciers advanced, before the Indus Valley (Kamp and Owen 2011).

In order to reassess the taxonomic relationships among the *A. roylei* species group, we sequenced the cytochrome b (*Cytb*) gene of our collected samples. The molecular test results aim to contribute to the delineating species boundaries and reveal the geographic distribution of the species within the *A. roylei* species group, specifically how the diversification of species relates to the mountains of the region. Our study included field measurement data (head-body/tail ratio) of the samples along with dental characters analyzed by our collaborator, Eve Rowland (Florida Museum of Natural History) to begin to identify the species on morphological criteria.

MATERIALS AND METHODS

Sampling and laboratory techniques.—Tissue samples utilized in this study (Fig. 1; Table 2) originated from a series of expeditions to Northern Pakistan undertaken by researchers at the University of Florida (UF) and University of Vermont (UVM), Charles Woods and C. William Kilpatrick respectively, from 1991-1999 (Woods and Kilpatrick, 1997). Dry skins and skulls were deposited at the Florida Museum of Natural History for further analysis. Due to the efficacy of ethanol as a chemical preservative at room temperature, tissue was preserved in a 95% ethanol solution (Kilpatrick 2002). These tissues were housed at the University of Vermont (UVM). Early in these expeditions, tissues from different individuals at the same locality would be housed in the same vial. All tissues in the vial would be assigned the same UVM tissue number. As a result, it is not clear which of the dry skins and skulls correspond to the specific individual analyzed. Samples were divided based on samples that I sequenced (n=83), samples determined by field measurements (n=93), and samples examined for dental morphological characteristics by Eve Rowland (n=118). A total of 32 sampling localities from Northern Pakistan are represented in these analyses (Fig. 1; Table 2).

Prior to DNA extraction, I soaked tissue in volumes of distilled water in order to remove excess ethanol and prevent degradation of soft tissue (Kilpatrick 2002). I sliced the tissue into smaller portions to increase surface area, and subsequently incubated overnight at 56°C with proteinase k (Kilpatrick 2002). I then performed DNA extractions of these specimens with the Gentra Puregene Mouse Tail Kit (QIAGEN-Germantown, MD).

Amplification of 751 base pair (bp) of the mitochondrial cytochrome b (*Cytb*) gene was performed through polymerase chain reaction (PCR) using Ready to Go PCR Beads (Illustra). I utilized two primer pairs CytbA to CytbE (Sullivan et al. 1997) for the amplification of one

fragment, and CytbBath3 (Dávalos and Jansa 2004) to Cytb752R (Tiemann-Boege et al. 2000) for the amplification of the second fragment. The established parameters for denaturing, annealing, and extension consisted of the following: 94 degrees (1 min), 50 degrees (1 min), and 72 degrees (1 min, 10 s – Norris et al. 2008). While these parameters demonstrated efficacy for the CytbA through CytbE fragment, they did not for CytbBath3 to Cytb752R. Through experimentation, we found that higher annealing temperatures (53°C) for CytbBath3 to Cytb752R gave a better yield for our PCR products. We sent the PCR products to the TACGen Sanger sequencing facility in Richmond, California to be sequenced. Additional sequences used in this study originate from GenBank (Table 3; Table 4) and were compared against the DNA sequences of the tissue samples sent for sequencing.

Phylogenetic analyses.—We assembled contigs using CodonCode Aligner 9.0.1 and aligned by eye in a nexus file. From the 120 individuals analyzed, 20 individuals comprised an outgroup with members not in the *Alticola* genus as well as an additional 11 individuals comprised an outgroup with members in the *Alticola* genus including *A. semicanus*, *A. stoliczkanus*, and *A. strelzovi* (Table 4). Our ingroup comprised of members of the *A. roylei* species group; 6 individuals downloaded from GenBank (Table 3) and the remaining 83 individuals were members of the *A. roylei* species group sequenced in this study (Table 2).

I utilized the jModeltest 2.1.7 (Darriba et al. 2012) to determine a best-fit model of molecular evolution with the GTR + I + Γ model of substitution. A phylogenetic tree was constructed with Beast 1.10.4 (Drummond and Rambaut 2007). A fossil calibration for the most recent common ancestor of *Alticola* was derived from Kohli et al. (2014). An exponential prior was applied where zero offset=1.5 mya, mean=1.1682 mya, and the upper 95th percentile=5.0 mya. The

BEAST analysis was set using a lognormal uncorrelated relaxed clock and a Coalescent Bayesian Skyline tree prior with 5 groups. The BEAST analysis was run for 100,000,000 generations, with trees sampled every 10,000 generations. I visualized this BEAST run in Tracer v1.7.1 (Rambaut et al. 2014) to determine burnin and ensure ESS values exceeded 300. I constructed a maximum clade credibility tree in TreeAnnotator with a burnin of 1,000 trees.

Morphological analyses.—The following field measurements of individual samples (n=93) were recorded by Charles Woods and C. William Kilpatrick: total length (TL), tail length (TA), hind-foot (HB), and ear length (EN). I utilized these field measurements to calculate the head-body length (HB), ratio of tail length to hindfoot (TA/HF), ratio of tail length to head-body (TA/HB), and ratio of ear to head-body (EN/HB). Identification of the species based on ratio of tail length to head-body followed a species key established by Kryštufek et al. (2017). A ratio of less than 30% for tail length to head-body was keyed as *A. albicauda*, while a ratio greater than 30% was keyed as either *A. argentatus* or *A. montosus* (Kryštufek et al. 2017) Eve Rowland classified individuals (n=118) based on molar characteristics as molar types A, B, C, and D, which correspond to *A. roylei*, *A. albicauda*, *A. argentatus*, and *A. montosus* respectively (Kryštufek et al. 2017). Eve Rowland further analyzed 13 individuals from locality Hushe Valley Gondogoro, on tail color and pelage color characters to classify individuals suspected to be members of *A. albicauda*.

RESULTS

Phylogenetic results.—Our phylogenetic analyses (Fig. 2) confirmed the *A. roylei* species group diverged from other species within the *Alticola* genus including *A. stoliczkanus, A. semicanus,*

and *A. strelzowi* 1.9 (95% highest posterior density [HPD]= 1.5-3.47) Mya. As we suspected, the *A. roylei* species group forms a monophyletic group (posterior probability value [PP] =1.0) that is sister to the aforementioned species within the *Alticola* genus (PP=0.87). The five clades (all with PP=1.0) within the *A. roylei* species group of interest to us are named based on their geographic distributions across various mountain ranges in Northern Pakistan; Hindu Kush Clade, Eastern Kohistan Clade, Karakoram Clade (excluding the Xinjiang and Turkmenistan samples, which are sister to this clade), Great Himalayan Clade, and Hushe Valley Clade.

Our results suggest that the Karakoram Clade is sister to the monophyletic group comprised of the Hindu Kush Clade and Hushe Valley Clade (PP=0.64); the three clades shared a recent common ancestor 1.07 (95%, 0.68-2.03) Mya. The Karakoram Clade diverged from the Turkmenistan sample 0.52 (95%, 0.26-0.97) Mya, and the last common ancestor of individuals within the Karakoram clade existed 0.1 (95%, 0.04-0.2) Mya. The sister relationship displayed between the Karakoram Clade and the Turkmenistan sample is poorly supported (PP=0.47), while (PP=1.0) for the monophyly of a clade that unites the Xinjiang sample with the Karakoram Clade and Turkmenistan sample. The Hindu Kush Clade and Hushe Valley Clade diverged from each other 0.60 (95%, 0.33-1.14) Mya, and the high nodal support (PP=1.0) indicates that these clades shared a common ancestor. The most recent common ancestor of individuals within the Hindu Kush Clade existed 0.36 (95%, 0.18-0.69) Mya, while the most recent common ancestor of individuals within the Hushe Valley clade existed much later 0.06 (95%, 0.01-0.14) Mya. The Great Himalayan Clade and Eastern Kohistan Clade are sister clades, however, nodal support is poor (PP=0.47). These clades last shared a common ancestor 0.97 (95%, 0.53-1.84) Mya. The most recent common ancestor for individuals within the Great Himalayan Clade existed 0.13

(95%, 0.05-0.27) Mya, and the most recent common ancestor of individuals within the Eastern Kohistan Clade existed much later 0.07 (95%, 0.02-0.14) Mya.

Morphological results.—Eve Rowland examined dental characters of 118 individuals (n=118) classified as either *A. roylei* (A), *A. albicauda* (B), *A. argentatus* (C), and *A. montosus* (D) (Table 5; Table 6). We calculated the percentage incidence of these molar types against our five mitochondrial clades. The Hindu Kush Clade is comprised of 70.8% individuals classified as *A. roylei* type, 8.3% *A. albicauda* type, 20.8% *A. argentatus* type, and no individuals classified under the *A. montosus* type. The Hushe Valley clade is comprised of 33.3% *A. roylei* type, 33.3% *A. argentatus* type, 33.3% *A. montosus* type, and no individuals classified under the *A. albicauda* type. The Karakoram Clade is comprised of 43.5% *A. roylei* type, 52.2% *A. argentatus* type, 4.3% *A. montosus* type, and no individuals classified under the *A. albicauda* type. The Great Himalayan Clade is comprised of 8% *A. roylei* type, 4% *A. albicauda* type, 40% *A. argentatus* type, and 48% *A. montosus* type. Lastly, the Eastern Kohistan Clade is comprised of 33.3% *A. roylei* type, 33.3 % *A. argentatus* type, and no individuals classified as either the *A. albicauda* or *A. montosus* type.

According to Kryštufek (2017), the head-body to tail ratio threshold further keys species types: a ratio (<30%) corresponds to the *albicauda* type and (>30%) corresponds to the *argentatus/montosus* type. An *albicauda* type displays characteristically shorter tails relative to the *argentatus/montosus* type (Kryštufek et al. 2017). I classified individuals within our five mitochondrial clades using this established standard (Table 5; Table 6). The following mitochondrial clades consist of individuals with only the *argentatus/montosus* type: the Karakoram Clade, the Hindu Kush Clade, and the Eastern Kohistan Clade. Only 2 *albicauda*

type individuals comprise the Great Himalayan Clade (4.8%) while 40 *argentatus/montosus* type individuals comprise the Great Himalayan Clade (95.2%). A similar pattern emerged in the Hushe Valley Clade: 83.3% of individuals displayed the *argentatus/montosus* type and 16.7% of individuals displayed the *albicauda* type. However, the mean head-body to tail ratio of individuals within the Hushe Valley Clade (0.322 ± 0.17 mm) is lower compared to the mean of the other mitochondrial clades (Table 7).

DISCUSSION

Morphological patterns of the clades.—Diagnostic morphological traits for the *A. roylei* species group (distinctive M^3 with 3-4 lingual salient angles, moderately long tail) characterize the group (Kryštufek et al. 2017), however, the subtle variations in the tail length and M^3 among *A. montosus*, *A. argentatus*, and *A. albicauda* may not characterize the individual species. The head-body to tail ratio threshold proposed by (Kryštufek et al. 2017) to distinguish between the *argentatus/montosus* type (>30%) and *albicauda* type (<30%) is not fully congruent for the corresponding mitochondrial clades (Fig. 3; Table 5; Table 6). We expected the Hushe Valley clade individuals to exhibit only *albicauda* type tails, and individuals of the Great Himalayan clade to exhibit only *montosus* type molars. The Hushe Valley clade consists of only one individual of the *albicauda* type (29.2%). The range of tail to head-body ratio of the individuals within the Hushe Valley clade (29.2%-34.3%) along with the calculated mean and standard deviation (0.322 $\pm$ 0.17 mm) suggest these individuals display relatively short tails. Our Karakoram clade in accordance with the proposed threshold consists of only the *argentatus/montosus* type (0.461 $\pm$ 0.032 mm). These individuals display relatively long tails

compared to the Hindu Kush clade (0.424 ± 0.033 mm), Eastern Kohistan Clade (0.357 ± 0.028 mm), and Great Himalayan clade (0.416 ± 0.055 mm) as well.

Similarities in the M^3 pattern of *A. argentatus*, *A. albicauda*, and *A. roylei* makes it difficult to differentiate among these species. However, the presence of an isolated antero-buccal triangle in *A. montosus* differentiates this species from the confluent antero-buccal triangle in the other species mentioned above (Kryštufek et al. 2017). Our results show that the Great Himalayan clade is comprised of more individuals that exhibit the *montosus* type molar (48%), though, a proportion of individuals also exhibit the *argentatus* type molar (40%) (Table 5; Table 6). The presence of multiple molar types within the Great Himalayan clade also including *A. albicauda* (4%) and *A. roylei* (8%) suggests the *montosus* type may not occur as frequently in *Alticola montosus* as expected by (Kryštufek et al. 2017). Additionally, the presence of the *roylei* type molar across all 5 mitochondrial clades may suggest that the M^3 pattern is an old character common to the *Alticola roylei* species group rather than a unique character that can be utilized to distinguish among species. Results of both tail length and M^3 pattern indicate morphological patterns rather than diagnostic morphological traits.

Molecular Data.—Tribe Myodini is comprised of seven genera which include *Alticola*, *Craseomys*, *Hyperacrius*, *Myodes, Caryomys, Eothenomys, and Aschizomys* (Pardiñas et al.2017). All genera are included in our phylogenetic analysis except *Aschizomys*, and *Alticola* (Table 4). *Eoethenomys*, *Hyperacrius*, *Craseomys*, *Caryomys*, and *Myodes* form a monophyletic group as expected (Kohli et al. 2014; Tang et al. 2018), but with weak nodal support (PP=0.6; Fig. 2). Monophyly of the *Alticola* genus (PP=0.87) further divides into three clades: *A.*

stoliczkanus species group, *A. roylei* species group, and the clade that contains both *A. semicanus* and *A. strelzovi*. Validity of the *A. roylei* species group is well-supported (PP=1).

Individuals of the *A. roylei* species group last shared a common ancestor (1.23 [95% HPD = 0.76-2.3] Mya) and shared a common ancestor with other members of the *Alticola* genus (1.9 [95% HPD = 1.5-3.47] Mya). The age of divergence between the Hindu Kush clade and the Hushe Valley clade (0.6 [95% HPD = 0.33-1.14] Mya), as well as the Great Himalayan clade and Eastern Kohistan clade (0.97 [95% HPD = 0.53-1.84] Mya), is similar to closely related species such as *Craseomys andersoni* and *C. smithii* (0.43 [95% HPD=0.17-0.85] Mya), *C. rufocanus* and *C.. shanseius* (0.38 [95% HPD=0.16-0.77] Mya), and *Myodes centralis* and *M. glareolus* (0.81 [95% HPD=0.4-1.61] Mya). Our nodal support values suggest that these 5 mitochondrial clades correspond to individual species (Fig. 2).

Geographic Distributions and Biogeography.—Individuals collected from the Hindu Kush clade inhabit the Hindu Kush mountain range (Fig. 3), specifically from a lower elevation in the Kurram Agency (3266 m) to regions in the Chitral District. The Kabul River does not act as a strong geographic barrier between Kurram Agency and the Chitral District, rather, the individuals that reside in the south are related to the individuals that reside in the north. Similar to patterns found in *Calomyscus*, individuals that occur in the Safed Koh mountain range are related to those north of the Kabul River (Weller 2019). A morphological trend that may differentiate individuals in this clade from the other 4 mitochondrial clades is the relatively larger size of these individuals (head and body=107.6 ± 7.6 mm; Table 7). According to Schlitter and Setzer (1973), the holotype for *Alticola roylei parvidens* occurs in N Dir, Dir State, West Pakistan located within our range for collected individuals. Moreover, Schlitter and Setzer

(1973) discover *A. r. parvidens* within the locality of Safed Koh, North West Frontier, a locality that encompasses our corresponding individuals in the Safed Koh mountain range. As the Hindu Kush mountains extend into Afghanistan, further sampling from the Afghanistan side of the mountains is needed. Based on morphological trends and geographic distributions, we hypothesize that the Hindu Kush clade corresponds to *Alticola parvidens*.

The Hushe Valley is located southwest of the high elevation K2 mountain in the Central Karakoram mountain range. High elevations characterize the area, and the complex glacial network extending from the northern areas of the Central Karakoram to the Indus River may contribute to the isolation of the Hushe Valley clade from the Karakoram clade. Morphological characters unique to the Hushe Valley clade such as relatively shorter tails (Table 5; Table 6) may have evolved in isolation as a result of these barriers. Despite the sister relationship (PP=1) between the Hushe Valley clade and Hindu Kush clade (Fig. 2) as well as relatively recent divergence time (0.6 [95% HPD=0.33-1.14] Mya) of these clades, the geographic distribution of the Hushe Valley clade and the Hindu Kush clade are independent of each other. Hindu Kush ranges occur westward of the Karakoram ranges. The holotype of *A. albicauda* occurs in Braludu, Baltistan, which is close to the Hushe Valley locality. Presence of shorter tails in these individuals and the geographic distribution give us reason to suggest that the Hushe Valley clade corresponds to *A. albicauda*.

Individuals from the Great Himalayan clade occur across the Himalayan range in Northern Pakistan, including the Nanga Parbat (Fig. 3). The event in which glaciers originating from Nanga Parbat advanced toward the Hunza Valley may contribute to the isolation observed between the Great Himalayan clade and the Karakoram clade (Owen et al. 2000). The Gilgit and Indus rivers further isolate the Great Himalayan clade from the Eastern Kohistan and Karakoram

clade. The early divergence of the Great Himalayan clade from the Eastern Kohistan clade (0.97 [95% HPD=0.53-1.84] Mya; Fig. 2) supports the idea of the independent evolution of the Great Himalayan clade. All individuals within the Great Himalayan clade diverged recently (0.13 [95% HPD=0.05-0.27] Mya) and have strong nodal support (PP=1). However, the strength of the sister relationship between the Great Himalayan clade and the Eastern Kohistan clade is weak (PP=0.47). More data are needed to determine which clade is most closely related to the Great Himalayan clade.

Presence of a greater proportion of the *montosus* type molars (48%) distinguish the Great Himalayan clade from the other mitochondrial clades (Table 5; Table 6), whereas less than 40% of individuals in all other mitochondrial clades exhibit the *montosus* type. The type locality of *A. montosus* (True, 1894) is poorly specified as "Central Kashmir, 11,000 feet", which could also apply to other mitochondrial clades or the species *A. roylei*. However, the presence of the *montosus* type molars along with the traditional range of *A. montosus* (Hinton 1926; Schwarz 1938; Musser and Carleton 2005; Kryštufek et al.2017; Pardiñas et al.2017) allow us to hypothesize that the Great Himalayan clade corresponds to *A. montosus*. It is important to note that the presence of *montosus* type molars is a morphological trend rather than a diagnostic morphological character per Kryštufek et al.(2017) as there are other types of molars within the Great Himalayan clade (Table 5; Table 6). The most notable type is the *argentatus* type (40%).

Our individuals collected from the Karakoram clade occurred in areas throughout the Karakoram mountain range including Hunza Valley, Gilgit District, Khunjerab Pass, and northeastern Chitral District (Fig. 3). Glaciers that originated in Hunza Valley advanced to the Gilgit and Indus valleys, and the Hunza Valley glacier reached the intersection between the Hunza River and Gilgit River (Kamp and Owen 2011). The Hunza, Gilgit, and Indus Rivers are

all confluent with respect to one another and surround the distribution of our collected individuals. However, the Hunza River does not act as an isolating barrier. Individuals of the Karakoram clade are found on both sides of the Hunza River Valley. The separate distributions of the Karakoram clade and the Great Himalayan clade may be due to the Indus and Gilgit Rivers and is further exacerbated by the glacier barriers. The longer tails characteristic of the Karakoram clade (46.7 ± 3.7 mm; Table 7) further distinguish it from the Great Himalayan clade (41.8 ± 5.3 mm) and the Eastern Kohistan clade (99.9 ± 10.5 mm).

Phylogenetic analyses support that individuals in our Karakoram clade are related (PP = 1; Fig. 2) to samples in Turkmenistan (*A. argentatus argentatus*) and Xinjiang (possibly *A. a. worthingtoni*). The nodal support for the sister relationship between the Karakoram clade and *A. a. argentatus* (Turkmenistan) is weak (PP=0.47), however, the nodal support for *A. a. worthingtoni* (Xinjiang) being related to both the Karakoram clade and *A. a argentatus* (Turkmenistan) is strong (PP=1). More sampling from across the range of *A. argentatus* is necessary to tease apart the relationships among these populations.

Since the Turkmenistan sample (*A. argentatus argentatus*) is the nominal subspecies of *A. a argentatus* as well as the Xinjiang sample (possibly *A. a. worthingtoni*), the strong nodal support of the Karakoram clade with these samples suggests that the Karakoram clade corresponds to species *Alticola argentatus*. However, the subspecies classification of the Karakoram clade is yet to be determined. The type locality provided by Scully (1880) as *Arvicola blanfordi* in "Gilgit, Kashmir" does not specify which side of the Gilgit Valley the individuals were collected. The northern shore of the Gilgit Valley may correspond to the Karakoram clade distribution while the southern shore of the Gilgit Valley may correspond to the distribution of the Eastern Kohistan clade. Another name, *Alticola glacialis* (Miller 1913), may

correspond to the Karakoram clade as well since the Chogo Lungma Glacier, Baltistan, Kashmir occurs within the distribution. If *blanfordi* Scully, 1880, is part of the Karakorum clade, it would be the appropriate name for subspecies. Otherwise *glacialis* Miller, 1913, is also available as the subspecies name.

As indicated by the name, the distribution of the Eastern Kohistan clade lies in the eastern Kohistan arc mountains (Fig. 3). Individuals from the Eastern Kohistan clade occupy valleys within the Diamir District, though 4 individuals from this clade occupy Lake Mahodand, Swat District, to the due west of the Kohistan arc mountain range. According to Kamp and Owen (2011), major glaciation events occurred in Swat Valley. These glaciation events likely isolated the Diamir District samples from the Swat District samples, however, the strong nodal support for the relationship among these individuals (PP=1; Fig. 2) indicates that consistently strong isolation did not take place. The Gilgit and Indus Rivers acted as strong isolating barriers for the independent evolution of the Karakoram clade, Great Himalayan clade, and Eastern Kohistan clade. Despite the geographical overlap between the Eastern Kohistan clade and the Hindu Kush clade, the clades last shared a common ancestor (1.23 [95% HPD=0.76-2.3] Mya) and display subtle differences in morphological characters. Individuals of the Eastern Kohistan clade exhibit smaller body sizes (99.9 ± 10.5 mm) and relatively short tails (35.4 ± 2.5 mm) compared to the large body sizes (107.9 ± 7.6 mm) and relatively longer tails (45.6 ± 3.0 mm) of the Hindu Kush clade individuals (Table 7).

The geographical overlap between the Eastern Kohistan clade and the Hindu Kush clade form a potential contact zone for the species at Lake Mahofand, Swat District (Fig. 3). We present two possibilities for the occurrence of both clades: a hybridization event or separate species present in sympatry but fully reproductively isolated. We observed further morphological

differences between individuals of the Eastern Kohistan clade and individuals of the Hindu Kush present at the contact zone: the ears of the Eastern Kohistan clade individuals are relatively smaller (14.5 ± 1.7 mm, $n = 4$) compared to the ears of the Hindu Kush individuals (16.5 ± 1.0 mm, $n = 4$); the head-body size of Eastern Kohistan individuals are smaller (98.5 ± 14.6 mm, $n = 4$) than Hindu Kush (104.0 ± 9.1 mm, $n = 4$); and the tails of Eastern Kohistan individuals are smaller (35.8 ± 1.7 mm, $n = 4$) than those from Hindu Kush (46.5 ± 4.2 mm, $n = 4$). In order to assess the possibilities for either, the use of multiple nuclear genes is necessary due to the higher nodal resolution of nuclear genes compared to mitochondrial genes (Tang et al. 2018). Future studies aim to replicate (Tang et al. 2018; Bauer 2019) and utilize the *Ghr* gene and *Rbp3* gene, which have been valuable in other studies of the Myodini tribe and other muroids (Kohli et al. 2014; Tang et al. 2018; Bauer 2019). Due to insufficient sampling and genetic data, we are unable to determine which of the two possibilities occurred.

Glaciation of the Hindu Kush, Karakoram, and Himalayan mountains occurred in the Late Quaternary period due to the influence of Milankovitch oscillations (100,000 years) driving the glacial and interglacial cycles (Barnosky 2001; Kamp and Owen 2011). Glaciers arose in the Northern Pakistan mountain ranges due to seasonal summer precipitation. Our five mitochondrial clades have persisted for (1.23 [95% HPD=0.76-2.3] Mya) during which multiple Milankovitch oscillations have occurred. Our lineages have persisted within the same geographic area. The Indus and Gilgit rivers still isolate the mitochondrial clades through glacial and interglacial cycles (Kamp and Owen 2011). Separate geographic distributions of the Hindu Kush and Eastern Kohistan clade may be due to the presence of glaciers at the Tangir or Swat river valleys during glacial cycles (Kamp and Owen 2011). However, the presence of the contact zone suggests that during interglacial cycles, the Hindu Kush clade and Eastern Kohistan clade were not as isolated

from each other. According to Barnosky (2005), most mammalian lineages persist for at least 1.5 Mya and survive these Milankovitch oscillations without demonstrating evolutionary responses in each cycle. It is likely that our mitochondrial clades utilized the considerable elevational differences inherent to the mountains of Northern Pakistan to migrate from unfavorable habitat to favorable habitat higher or lower without traveling long distances.

ACKNOWLEDGEMENTS

I would like to thank Dr. Ryan Norris for serving as an incredible mentor to me and giving me an opportunity to work with the samples. I would not be able to complete this project without his dedication and hard work. C. W Kilpatrick and C.A Woods collected these samples during the (1992-1998) expeditions. From the Florida Museum of Natural History, Eve Rowland analyzed morphological data for my samples which allowed me to expand my project. Verity Mathis was instrumental in tracking down samples and conducting morphological analyses. Kevin Scott provided valuable geographic data by compiling type localities of Northern Pakistan. Jacqi Bishop performed DNA extractions on a few of the samples. Lastly, I would like to thank members of the Norris Lab for supporting me throughout this project. Reading and reviewing the theses of other members of the Norris lab including Rachel Crites, Amanda Weller, and George Bauer allowed me to improve upon my thesis. Kedar Roderick, Kylie Alvarado, and Anna Walker have been wonderful in supporting my project and providing feedback. Lastly, I would like to thank my family and friends for encouraging my development as a researcher.

LITERATURE CITED

BARNOSKY, A.D. 2001. Distinguishing the effects of the Red Queen and Court Jester on Miocene mammal evolution in the Northern Rocky Mountains. Journal of Vertebrate Paleontology 21: 172-185.

BAUER, G. 2019. Do forest refugia and riverine barriers promote genetic diversity among species in the *Hybomys* division? Undergraduate thesis at The Ohio State University.

DARRIBA, D., G.L. TABOADA, R. DOALLA AND D. POSADA. 2012. jModelTest 2: more models, new heuristics and parallel computing. Nature Methods 9:772.

DÁVALOS, L.M. AND S. A. JANSA. 2004. Phylogeny of the Lonchophyllini (Chiroptera: Phyllostomidae). Journal of Mammalogy 85: 404–413.

DRUMMOND, A.J., AND A. RAMBAUT. 2007. BEAST: Bayesian evolutionary analysis by sampling trees. BMC Evolutionary Biology 7: 214.

HINTON, M.A.C. 1926. Monograph of the voles and lemmings (Microtinae) living and extinct. British Museum (Natural His- tory), London, 1:1-488.

JORDAN, M. AND S. MOLUR. 2016. *Alticola albicaudus*. The IUCN Red List of Threatened Species. Downloaded on 11 July 2020.

KAMP, U. AND L. A OWEN. 2011. Chapter 66: Late Quaternary Glaciation of Northern Pakistan. Developments in Quaternary Science 15: 909-927.

KILPATRICK, C.W. 2002. Noncryogenic preservation of mammalian tissue for DNA extraction: An assessment of storage methods. Biochemical Genetics 40:53–62.

KOHLI, B.A., K.A SPEER, C.W KILPATRICK, N. BATSAIKHAN, D. DAMDINBAZA, J.A COOK. 2014. Multilocus systematics and non-punctuated evolution of Holarctic Myodini (Rodentia: Arvicolinae). Molecular Phylogenetics and Evolution 76: 18-29.

KRYŠTUFEK, B., G. I. SHENBROT, J. GREGORI, P. BENDA, R. HUTTERER. 2017. Taxonomic and geographic setting of Royle's mountain vole *Alticola roylei* revisited. Mammalia 81: 503-511.

LEBEDEV, V.S., A. A. BANNIKOVA, A.S TESAKOV, N.I ABRAMSON. 2007. Molecular phylogeny of the genus *Alticola* (Cricetidae, Rodentia) as inferred from the sequence of the cytochrome b gene. Zoologica Scripta 36: 547-563.

MOLUR, S. 2016a. *Alticola argentatus*. The IUCN Red List of Threatened Species. Downloaded on 11 July 2020.

MOLUR, S. 2016b. *Alticola montosa*. The IUCN Red List of Threatened Species. Downloaded on 11 July 2020.

MUSSER, G.G. AND M.D. CARLETON. 2005. Superfamily Muroidea. Pp. 894–1531 in Mammal species of the world: a taxonomic and geographic reference. 3rd edition (D. E. Wilson and D. M. Reeder, eds.). Johns Hopkins University Press. Baltimore, Maryland.

NADACHOWSKI, A. AND J. I MEAD. 1999. Alticola argentatus. Mammalian Species 625: 1-4.

NORRIS, R. W., C. A. WOODS, AND C. W. KILPATRICK. 2008. Morphological and molecular definition of *Calomyscus hotsoni* (Rodentia: Muroidea: Calomyscidae). Journal of Mammalogy, 89:306-315.

OWEN, L.A., SCOTT, C.H., DERBYSHIRE, E. 2000. The Quaternary glacial history of Nanga Parbat. Quaternary International 65: 63–79.

PARDIÑAS, U. F. J., D. RUELAS, J. BRITO, L. C. BRADLEY, R. D. BRADLEY, N. ORDÓÑEZ GARZA, B. KRYŠTUFEK, J. A. COOK, E. CUÉLLAR, SOTO, J. SALAZAR-BRAVO, G. I. SHENBROT, E. A. CHIQUITO, A. R. PERCEQUILLO, J. R. PRADO, R. HASLAUER, J. L. PATTON, AND L. LEÓN-PANIAGUA. 2017. Family Cricetidae (True hamsters, voles, lemmings, and New World rats and mice). Pp. 204-535 in Handbook of the Mammals of the World. Vol. 7, Rodents II (D.E. Wilson, T.E. Lacher, Jr., and R.A. Mittermeier RA eds.). Lynx Edicions, Barcelona.

PHILLIPS, C. J. 1969. Review of Central Asian Voles of the Genus *Hyperacrius*, with comments on Zoogeography, Ecology, and Ectoparasites. Journal of Mammalogy 50: 457-474.

RAMBAUT, A., M.A. SUCHARD, D. XIE, AND A.J. DRUMMOND. 2014. Tracer v1.6. <http://beast.bio.ed.ac.uk/Tracer>

ROBERTS, T.J. 1997. The mammals of Pakistan, revised edition. Oxford University Press, Oxford.

SCHLITTER, D.A. AND H.W SETZER. 1973. New Rodents (Mammalia: Cricetidae, Muridae) from Iran and Pakistan. Proceedings of the Biological Society of Washington 86: 163-174.

SCHWARZ, E. 1938. On Mountain-Voles of the Genus *Alticola* Blanford: a Taxonomic and Genetic Analysis. Proceedings of the Zoological Society of London B 108: 663-668.

SCULLY, J. 1880. Description of a new species of *Arvicola* from Gilgit. Annals and Magazine of Natural History, Series 5:399- 400.

SULLIVAN, J., J.A. MARKERT, AND C. W. KILPATRICK. 1997. Phylogeography and molecular systematics of the *Peromyscus aztecus* group (Rodentia: Muridae) inferred using parsimony and likelihood. Systematic Biology 46: 426–440.

TANG, M.K., W. JIN, Y. TANG, C.C YAN, R.W MURPHY ET AL. 2018. Reassessment of the taxonomic status of *Craseomys* and three controversial species of *Myodes* and *Alticola* (Rodentia: Arvicolinae). Zootaxa 4429: 1-52.

TIEMANN-BOEGE, I., C. W. KILPATRICK, AND R.D. BRADLEY. 2000. Molecular Phylogenetics of the *Peromyscus boylii* species group (Rodentia: Muridae) based on mitochondrial cytochrome *b* sequences. Molecular Phylogenetics and Evolution 16:366-378.

TRUE, F.W. 1894. Notes on mammals of Baluchistan and Vale of Kashmir presented to the National Museum by Dr. W. L. Abbott. Proceedings of the United States National Museum, 17:1-16.

WELLER, A. 2019. Systematics and ecology of the brush-tailed mice, *Calomyscus*, in and around Pakistan based on the *Rbp3* gene. Undergraduate thesis at The Ohio State University.

WOODS, C.A. AND C.W KILPATRICK. 1997. Biodiversity of Small Mammals in the Mountains of Pakistan. Pp. 437-467 in Biodiversity of Pakistan. (Mufti, S.A., C. A. Woods, and S. A. Hasan, eds.). Pakistan Museum of Natural History Islamabad.

FIGURE LEGENDS

FIGURE 1- Geographic distributions of the *Alticola roylei* species group. The blue and yellow shading represents the distributions of *Alticola albicauda* and *Alticola montosus* respectively (Jordan and Molur 2016; Molur 2016b). The black dots represent our samples, and the white boxes represent type localities for the species. Species currently recognized in *A. roylei* species group are *A. argentatus* (type locality in Tajikistan) including synonyms bl=*blanfordi*, gl=*glacialis*, la=*lahulius*, pa=*parvidens*; A. *montosus* (type locality = "Central Kashmir" not shown) incl. im=*imitator*; *A. albicauda* (al) incl. ac=*acmaeus*; *A. roylei* (type locality = "Kashmir"), which is mostly outside map. Kevin Scott was vital in compiling this map with localities to be used in my analysis. Our black dot with the yellow border is presumed to be related to the other *A. montosus* samples, however, it falls outside of the typical distribution. Dotted black border encompasses the range for species *Alticola argentatus*, and at least two of its subspecies (*A. a. blanfordi* and *A. a parvidens*) (Molur 2016a).

FIGURE 2-The Bayesian tree contains our five mitochondrial clades including the Karakorum clade (orange), Hindu Kush clade (purple), Hushe Valley clade (blue), Great Himalayan clade (yellow), and Eastern Kohistan clade (red). Blue bars represent the 95% confidence interval with respect to divergence times, and the numbers represent the posterior probability values. The triangles indicate the samples collapsed into the various clades.

FIGURE 3-Geographic distributions of the *Alticola roylei* species group based on our molecular clades. As stated in Figure 1, the black dots represent our samples. The empty blue, yellow, and

black boundaries represent the old boundaries of *A. albicauda*, *A. montosus*, *A. argentatus*. The black dot with the blue border represents the Hushe Valley clade.

Figure 1

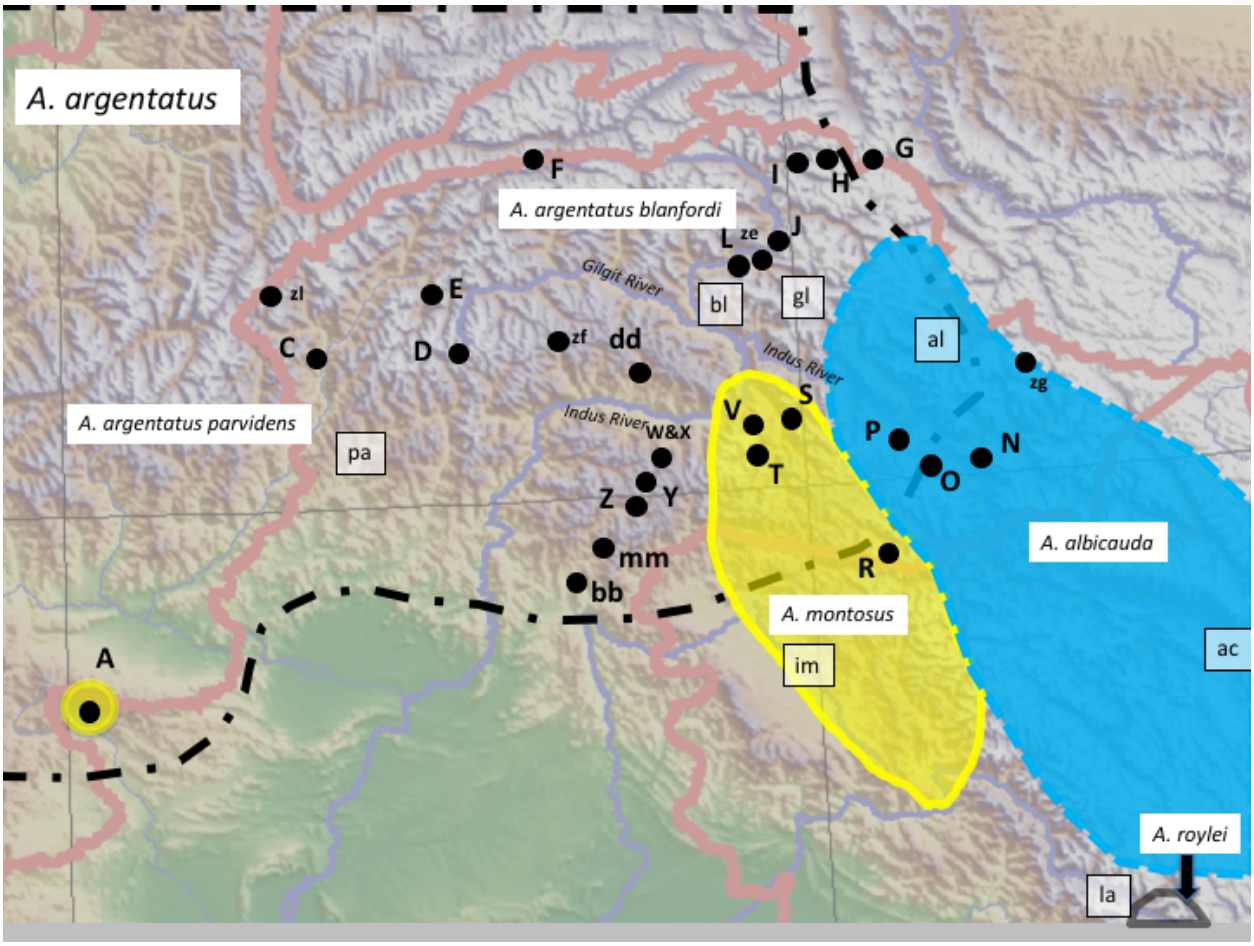
A. argentatus
A. argentatus blanfordi
A. argentatus parvidens
A. albicauda
A. montosus
A. roylei
Gilgit River
Indus River
Indus River
pa
bl
gl
al
im
ac
la
A
C
D
E
F
G
H
I
J
L
S
T
V
W&X
Y
Z
bb
dd
mm
N
O
P
R
zf
zg
zl
ze

Figure 2

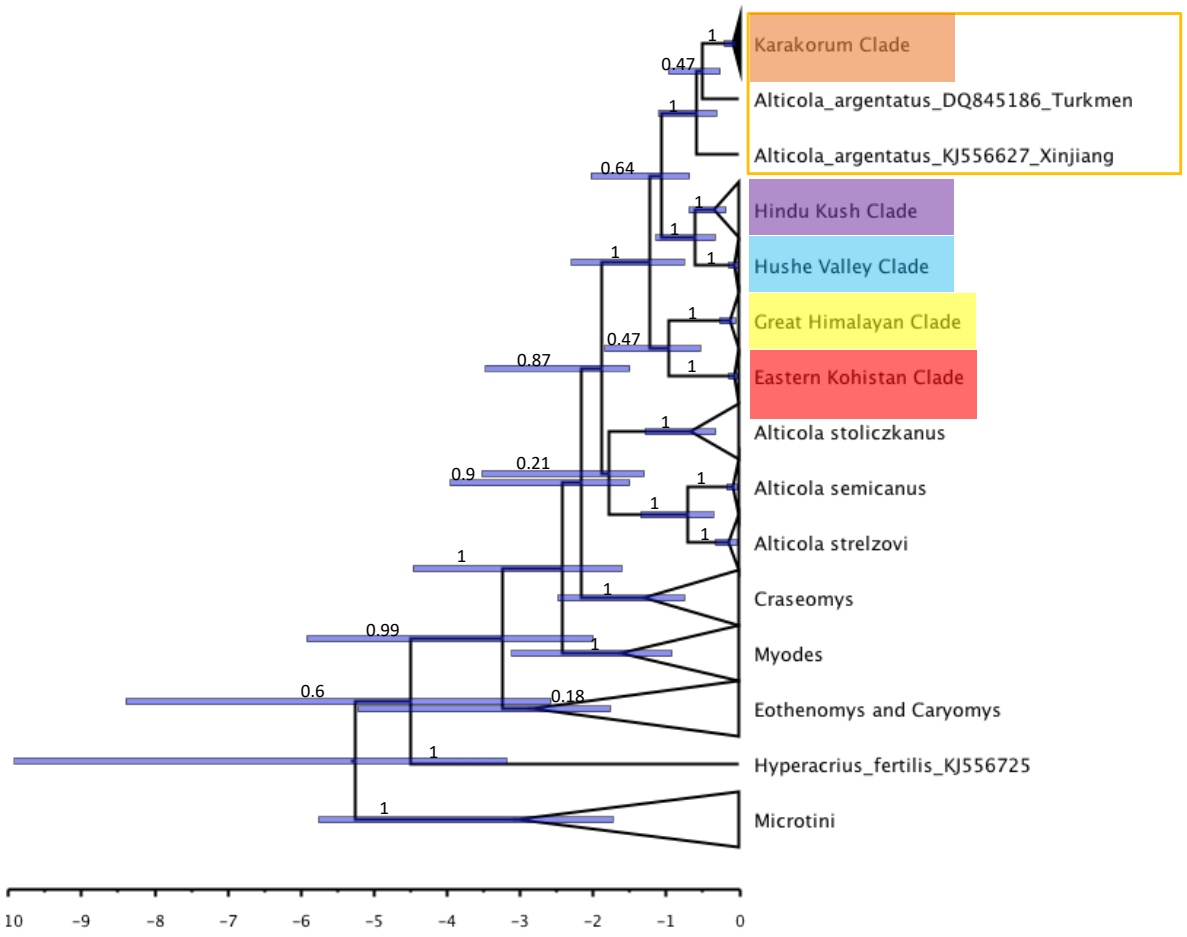
Karakorum Clade
Alticola_argentatus_DQ845186_Turkmen
Alticola_argentatus_KJ556627_Xinjiang
Hindu Kush Clade
Hushe Valley Clade
Great Himalayan Clade
Eastern Kohistan Clade
Alticola stoliczkanus
Alticola semicanus
Alticola strelzovi
Craseomys
Myodes
Eothenomys and Caryomys
Hyperacrius_fertilis_KJ556725
Microtini
10
-9
-8
-7
-6
-5
-4
-3
-2
-1
0

Figure 3

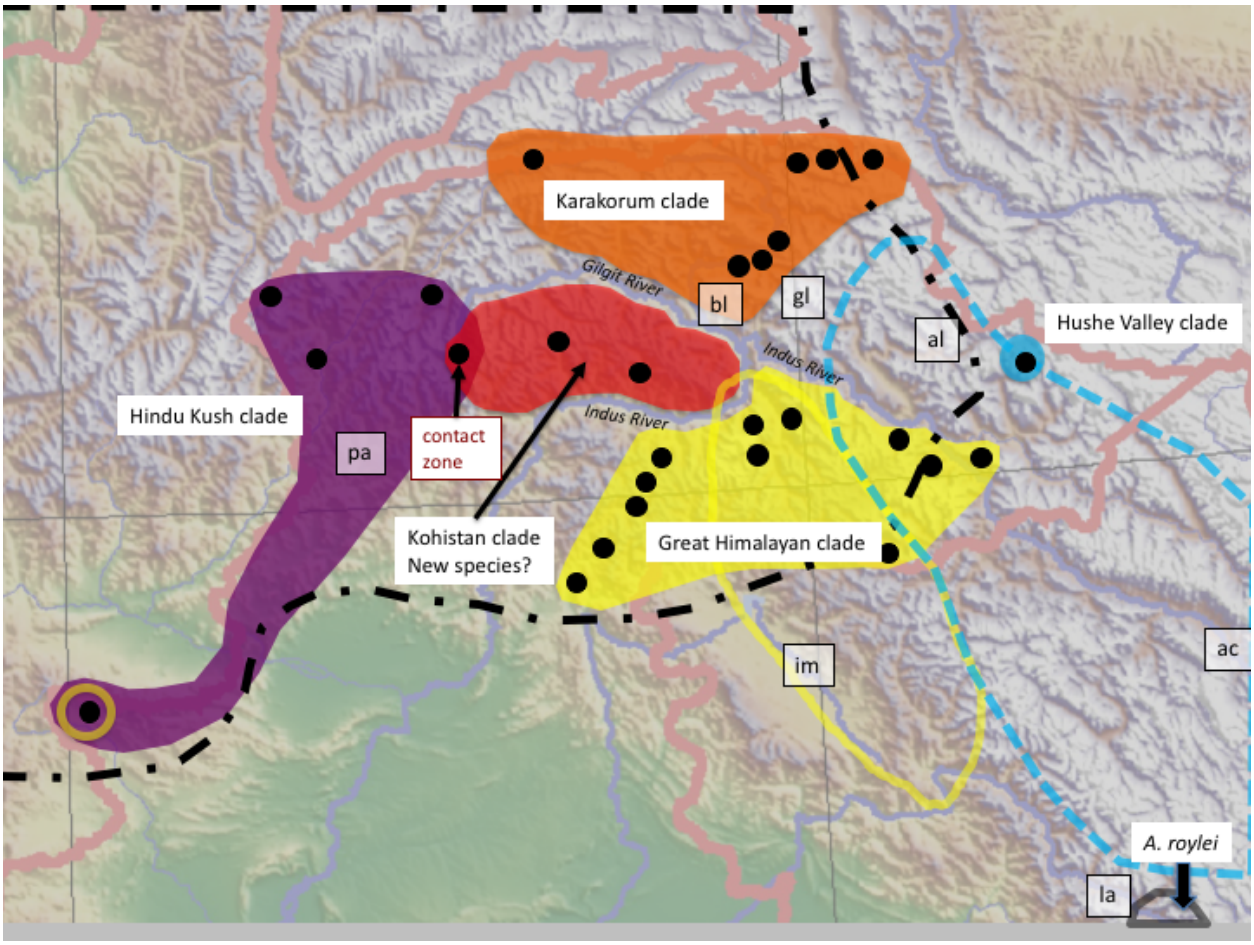
Karakorum clade
Gilgit River
bl
gl
al
Hushe Valley clade
Indus River
Hindu Kush clade
pa
contact zone
Indus River
Kohistan clade
New species?
Great Himalayan clade
im
ac
A. roylei
la

TABLE 1—. The conventional diagnostic characteristics for species in the *Alticola roylei* species group (Kryštufek et al. 2017).

Species	**Antero-buccal triangle in M^3 tooth BT1 large and isolated from the anterior loop**	**Tail relatively shorter (< 30% of head and body length)**
A. roylei		
A. argentatus		
A. montosus	X	
A. albicauda		X

TABLE 2.—. Identification of samples that I sequenced at the Ohio State University at Lima with locality information determined during field expeditions (1992-1998) undertaken by C.W Kilpatrick and C.A Woods. Map symbols correspond to Figure 1. All localities are in Pakistan.

Mt Clade	Locality	Map symbol	UVM tissue (#)
E. Kohistan	Gilgit-Baltistan, Diamer District, Tangir Valley, Satev, 2900 m	zf	876, 877
E. Kohistan	Gilgit-Baltistan, Diamer District, Khanbari Valley, Saromoos, 2950 m	dd	852, 853
E. Kohistan	Gilgit-Baltistan, Diamer District, Khanbari Valley, Kalidatt, 3300 m	dd	861
E. Kohistan and H. Kush	Khyber Pakhtunkhwa, Swat District, Lake Mahodand, 2980 m	D	654, 655, 664, 665
G. Himalayan	Gilgit-Baltistan, North Slope, Nanga Parbat	V	444, 445, 446
G. Himalayan	Gilgit-Baltistan, Diamer District, Babusar Village, 10,220 ft	W	604, 605, 606, 607, 608, 617
G. Himalayan	Gilgit-Baltistan, Baltistan District, Shoshar Lake, 13,616 ft	P	649
G. Himalayan	Khyber Pakhtunkhwa, Sari	zk	284, 454
G. Himalayan	Khyber Pakhtunkhwa, Palas Valley, Khubkot Nulla, 2330 m	bb	491
G. Himalayan	Khyber Pakhtunkhwa, Palas Valley, Guta Bek, 2700 m	bb	496
G. Himalayan	Khyber Pakhtunkhwa, Mansehra District, Babusar Top, 4070 m	X	721
G. Himalayan	Khyber Pakhtunkhwa, Mansehra District, Bugla, 9000 ft	zh	586
G. Himalayan	Khyber Pakhtunkhwa, Hazar District, Besal, 3400 m	Y	439
G. Himalayan	Khyber Pakhtunkhwa, Mansehra District, Burawai, 3053 m	Z	715, 723
G. Himalayan	Gilgit-Baltistan, Diamer District, Terashing, 9617 ft	T	628, 630
G. Himalayan	Gilgit-Baltistan, Diamer District, Bonardas Valley, Paloi, 2900 m	zj	866
G. Himalayan	Gilgit-Baltistan, Baltastan District, Gulteri, Sufaid Nala, 3650 m	R	705, 706
G. Himalayan	Gilgit-Baltistan, Parishing Valley	S	397
G. Himalayan	Gilgit-Baltistan, Shatung La, 4030 m	O	403
G. Himalayan	Gilgit-Baltistan, Satpara Darei, 3000m	N	407
H. Valley	Gilgit-Baltistan, Ganche District, Hushey Valley Gondogoro, 3750 m	zg	521, 522, 528, 529
H. Kush	Khyber Pakhtunkhwa, Kurram Agency, Zundialai, 3266 m	A	1479, 1478, 1477, 1474, 1475
H. Kush	Khyber Pakhtunkhwa, Kurram Agency, Upper Zundialai, 3386 m	A	1480, 148, 1485, 1486
H. Kush	Khyber Pakhtunkhwa, Chitral District, Sundalai, 2950 m	C	1225, 1226, 1227, 1228
H. Kush	Khyber Pakhtunkhwa, Chitral District, Sherkandah, 7500 ft	zl	413

H. Kush	Khyber Pakhtunkhwa, Chitral District, 1 km W Sherkandah	zl	420
H. Kush	Khyber Pakhtunkhwa, Chitral District, Shah Sadeum	zi	418
H. Kush	Khyber Pakhtunkhwa, Chitral District, Shandur Pass, 3700 m	E	429
H. Kush	Khyber Pakhtunkhwa, Swat District, Lake Mahodand, 2980 m	D	663, 666, 667, 668
Kar.	Khyber Pakhtunkhwa, Chitral District, Kishmanja, 3188 m	F	1428, 1429, 1430, 1431
Kar.	Gilgit-Baltistan, Gilgit District, Gulmit, 2670 m	J	694, 687, 688, 691, 690, 689, 692, 693
Kar.	Khyber Pakhtunkhwa, Chitral District, Kishmanja, 3188 m	ze	1570, 1571, 1572
Kar.	Gilgit-Baltistan, Truken, 3500 m	H	406 ,447, 448, 449, 450
Kar.	Gilgit-Baltistan, Gilgit District, Nagar, Rakaposhi Base Camp (Tagaferi), 3500 m	L	695
Kar.	Gilgit-Baltistan, Gilgit District, Khunjerab Pass, 4520 m	I	537

TABLE 3.—. Identification of sequences downloaded from GenBank with localities (Kohli et al. 2014; Lebedev et al. 2007).

Mt. Clade	**Locality**	**GenBank #**	**Specimen#**
Kar.	Pakistan, Gilgit-Baltistan, Truken, 3550 m	KJ556726	UVM406
Kar.	Pakistan, Gilgit-Baltistan, Truken, 3500 m	KJ556729	UVM447
H. Kush	Pakistan, specific locality is unclear	KJ556727	UVM431
G. Himalayan	Pakistan, Khyber Pakhtunkhwa, Hazar District, Hazar District	KJ556728	UVM439
A. argentatus	Turkmenistan, Kugitang	DQ845186	N/A
A. argentatus	Xinjiang, Xinjiang, 3.9 km N., 28.3 km E. Narati, 43.3671 N 84.3595 E	KJ556627	MSB15876

TABLE 4.—. GenBank accession numbers for sequences used in this study. *The asterisks show the classification of these samples according to Kohli et al. (2014). My results indicate that this designation is not supported by either morphology or genetics. These samples are part of the Karakorum clade.

Species	**Accession # for *Cytb***
Alexandromys fortis (Microtini)	NC015243
Alexandromys kikuchii (Microtini)	NC003041
Microtus levis (Microtini)	NC008064
Neodon irene (Microtini)	NC016055
Hyperacrius fertilis	KJ556725
Caryomys eva	HM165401
Caryomys inez	HM165385
Eothenomys chinensis	HM165434
Eothenomys custos	HM165408
Eothenomys melanogaster	HM165399
Craseomys andersoni	AB037303
Craseomys regulus	DQ138124
Craseomys smithii	AB037308
Myodes californicus	AY309422
Myodes centralis	KY968281
Myodes gapperi	AF272639
Myodes glareolus	AY309421
Craseomys rex	AB565455
Craseomys rufocanus	KY968275
Craseomys shanseius	KY968266
Alticola strelzovi	DQ845190
Alticola strelzovi	KJ556696
Alticola semicanus	DQ845187
Alticola semicanus	KJ556617
Alticola semicanus	KJ556620
Alticola stoliczkanus	KY968270
Alticola stoliczkanus	KY968271
Alticola stoliczkanus	KY968272
Alticola stoliczkanus	KY968268
Alticola stoliczkanus	MF040961
Alticola stoliczkanus (stracheyi)	KY968269
Alticola montosus	KJ556728
*Alticola albicauda**	KJ556726
*Alticola albicauda**	KJ556729
Alticola argentatus	KJ556727
Alticola argentatus argentatus (Turkemenistan)	KJ556627
Alticola argentatus worthingtoni (Xinjiang)	DQ845186

TABLE 5.—. Identification of samples that I sequenced at the Ohio State University at Lima based on measurement (tail length/head-body ratio), tooth characters, and mitochondrial clade. Dental characters were coded by Eve Rowland at UF based on Fig. 3 of Kryštufek et al. (2017). A tail/head-body ratio < 30% indicates *A. albicauda* according to Kryštufek et al. (2017). A tail/head-body ratio > 30% indicates *A. argentatus* or *A. montosus* (abbreviated *argen/mont*). These are UVM tissue numbers that correspond to only one individual each.

UVM tissue #	Field ID	Measurement Ratio	Measurement Species ID	Tooth Species ID	Mt Clade
1474	P-7578	N/A	N/A	*roylei*	H. Kush
1477	P-7586	N/A	N/A	roylei	H. Kush
1478	P-7587	N/A	N/A	*roylei*	H. Kush
1479	P-7588	N/A	N/A	*albicauda*	H. Kush
1480	P-7591	N/A	N/A	*roylei*	H. Kush
1481	P-7592	N/A	N/A	*roylei*	H. Kush
1485	P-7597	N/A	N/A	*roylei*	H. Kush
1486	P-7598	N/A	N/A	*roylei*	H. Kush
1225	P-6511	0.431	*argen/mont*	*roylei*	H. Kush
1226	P-6512	0.411	*argen/mont*	*roylei*	H. Kush
1227	P-6513	0.455	*argen/mont*	*albicauda*	H. Kush
1228	P-6514	0.474	*argen/mont*	*roylei*	H. Kush
654	P-3153	0.364	*argen/mont*	*argentatus*	E. Kohistan
655	P-3154	0.422	*argen/mont*	*argentatus*	E. Kohistan
663	P-3187	0.436	*argen/mont*	*argentatus*	Kar.
664	P-3247	0.322	*argen/mont*	*argentatus*	E. Kohistan
665	P-3248	0.362	*argen/mont*	*argentatus*	E. Kohistan
666	P-3249	0.479	*argen/mont*	*argentatus*	H. Kush
667	P-3250	0.398	*argen/mont*	*roylei*	H. Kush
668	P-3251	0.480	*argen/mont*	*argentatus*	H. Kush
429	P-836	0.421	*argen/mont*	*roylei*	H. Kush
1428	P-10036	N/A	N/A	*argentatus*	Kar.
1429	P-10037	N/A	N/A	*argentatus*	Kar.
1430	P-10038	N/A	N/A	*roylei*	Kar.
1431	P-10041	N/A	N/A	*argentatus*	Kar.
447	P-2094	0.500	*argen/mont*	*argentatus*	Kar.
448	P-2095	0.452	*argen/mont*	*argentatus*	Kar.
449	P-2096	0.480	*argen/mont*	*roylei*	Kar.
450	P-2097	0.406	*argen/mont*	*roylei*	Kar.
687	P-3295	0.509	*argen/mont*	*roylei*	Kar.
663	P-3187	0.436	*argen/mont*	*argentatus*	H. Kush
688	P-3296	0.450	*argen/mont*	*argentatus*	Kar.
689	P-3297	0.476	*argen/mont*	*argentatus*	Kar.
690	P-3298	0.476	*argen/mont*	*argentatus*	Kar.
691	P-3299	0.477	*argen/mont*	*roylei*	Kar.
692	P-3300	0.434	*argen/mont*	*roylei*	Kar.
693	P-3301	0.474	*argen/mont*	*argentatus*	Kar.
694	P-3302	0.484	*argen/mont*	*roylei*	Kar.
695	P-3308	0.481	*argen/mont*	*argentatus*	Kar.
649	P-2835	0.385	*argen/mont*	N/A	G. Himalayan
705	P-3319	0.364	*argen/mont*	*argentatus*	G. Himalayan

706	P-3320	0.340	*argen/mont*	N/A	G. Himalayan
628	P-2809	0.438	*argen/mont*	*argentatus*	G. Himalayan
630	P-2811	0.376	*argen/mont*	N/A	G. Himalayan
444	P-801	0.348	*argen/mont*	N/A	G. Himalayan
446	P-804	0.412	*argen/mont*	*argentatus*	G. Himalayan
604	P-2772	0.467	*argen/mont*	N/A	G. Himalayan
605	P-2773	0.448	*argen/mont*	*roylei*	G. Himalayan
606	P-2774	0.429	*argen/mont*	N/A	G. Himalayan
607	P-2775	0.461	*argen/mont*	*montosus*	G. Himalayan
608	P-2776	0.402	*argen/mont*	N/A	G. Himalayan
617	P-2785	0.429	*argen/mont*	N/A	G. Himalayan
723	P-3231	0.438	*argen/mont*	*albicauda*	G. Himalayan
496	P-2245	N/A	N/A	N/A	G. Himalayan
853	P-2302	0.346	*argen/mont*	*roylei*	E. Kohistan
1570	P-1	N/A	N/A	N/A	Kar.
1571	P-2	N/A	N/A	N/A	Kar.
1572	P-3	N/A	N/A	N/A	Kar.
876	P-2349	0.351	*argen/mont*	*argentatus*	E. Kohistan
877	P-2350	0.350	*argen/mont*	roylei	E. Kohistan
586	P-2743	N/A	N/A	N/A	G. Himalayan
866	P-2324	0.358	*argen/mont*	*montosus*	G. Himalayan
420	P-901	0.367	*argen/mont*	*argentatus*	H. Kush
445	P-803	0.407	*argen/mont*	N/A	G. Himalayan
521	P-2400	0.318	*albicauda*	*argentatus*	H. Valley
522	P-2401	0.276	*albicauda*	*roylei*	H. Valley
1475	P-7579	N/A	N/A	N/A	H. Kush

TABLE 6.—. Identification of samples that I sequenced at the Ohio State University at Lima based on Measurement (Tail length/Head-Body Ratio), Tooth characters, and Mitochondrial Clade. Dental characters were coded by Eve Rowland at UF based on Fig. 3 of Kryštufek et al. (2017). A tail/head-body ratio < 30% indicates *A. albicauda* according to Kryštufek et al. (2017). A tail/head-body ratio > 30% indicates *A. argentatus* or *A. montosus* (abbreviated *argen/mont*).These are UVM tissue numbers where one tissue vial and number corresponds to multiple individuals.

UVM tissue #	Field ID	Measurement Ratio	Measurement Species ID	Tooth Species ID	Mt Clade
408 (1)	P-2098	0.416	*argen/mont*	N/A	Kar.
408 (2)	P-2099	0.429	*argen/mont*	*montosus*	Kar.
406 (1)	P-2108	0.505	*argen/mont*	N/A	Kar.
406 (2)	P-2109	0.459	*argen/mont*	N/A	Kar.
406 (3)	P-2112	0.485	*argen/mont*	*argentatus*	Kar.
406 (4)	P-2113	0.400	*argen/mont*	*roylei*	Kar.
537 (1)	P-2444	N/A	N/A	*roylei*	Kar.
537 (2)	P-2445	N/A	N/A	*roylei*	Kar.
407 (1)	P-2075	0.495	*argen/mont*	*montosus*	G. Himalayan
407 (2)	P-2089	0.489	*argen/mont*	*montosus*	G. Himalayan
407 (3)	P-2088	0.421	*argen/mont*	*argentatus*	G. Himalayan
407 (4)	P-2090	0.563	*argen/mont*	*montosus*	G. Himalayan
407 (5)	P-2084	N/A	N/A	*montosus*	G. Himalayan
403(1)	P-767	0.396	*argen/mont*	*montosus*	G. Himalayan
403 (2)	P-768	0.299	*albicauda*	*montosus*	G. Himalayan
403 (3)	P-769	0.299	*albicauda*	*montosus*	G. Himalayan
403 (4)	P-770	0.361	*argen/mont*	*montosus*	G. Himalayan
403 (5)	P-771	0.413	*argen/mont*	*montosus*	G. Himalayan
721 (1)	P-3228	0.361	*argen/mont*	N/A	G. Himalayan
721 (2)	P-3229	0.452	*argen/mont*	N/A	G. Himalayan
439 (1)	P-1226	0.392	*argen/mont*	*albicauda*	G. Himalayan
439 (2)	P-1227	0.380	*argen/mont*	*argentatus*	G. Himalayan
439 (3)	P-1229	0.400	*argen/mont*	*argentatus*	G. Himalayan
715 (1)	P-3189	0.455	*argen/mont*	N/A	G. Himalayan
715 (2)	P-3226	0.415	*argen/mont*	N/A	G. Himalayan
852 (1)	P-2301	0.360	*argen/mont*	*argentatus*	E. Kohistan
852 (2)	P-2303	0.333	*argen/mont*	*roylei*	E. Kohistan
418 (1)	P-1004	N/A	N/A	*roylei*	H. Kush
418 (2)	P-1017	N/A	N/A	*roylei*	H. Kush
418 (3)	P-1018	N/A	N/A	*roylei*	H. Kush
284 (1)	P-84	0.481	*argen/mont*	N/A	G. Himalayan
284 (2)	P-85	0.423	*argen/mont*	N/A	G. Himalayan
284 (3)	P-86	0.504	*argen/mont*	N/A	G. Himalayan
284 (4)	P-87	0.526	*argen/mont*	N/A	G. Himalayan
454 (1)	P-986	N/A	N/A	*argentatus*	G. Himalayan
454 (2)	P-987	N/A	N/A	*argentatus*	G. Himalayan
413 (1)	P-845	0.380	*argen/mont*	N/A	H. Kush
413 (2)	P-846	0.407	*argen/mont*	*roylei*	H. Kush
413 (3)	P-881	0.395	*argen/mont*	*argentatus*	H. Kush
413 (4)	P-882	0.402	*argen/mont*	*roylei*	H. Kush
413 (5)	P-883	0.431	*argen/mont*	*argentatus*	H. Kush

528 (1)	P-2409	0.306	*argen/mont*	*roylei*	H. Valley
528 (2)	P-2410	0.318	*argen/mont*	*argentatus*	H. Valley
529 (1)	P-2411	0.315	*argen/mont*	*montosus*	H. Valley
529 (2)	P-2412	0.276	*argen/mont*	*montosus*	H. Valley
397 (1)	P-712	N/A	N/A	N/A	*G. Himalayan*
397 (2)	P-713	0.396	*argen/mont*	*argentatus*	*G. Himalayan*
397 (3)	P-714	N/A	N/A	*montosus*	*G. Himalayan*
397 (4)	P-721	0.407	*argen/mont*	N/A	*G. Himalayan*
397 (5)	P-727	0.397	*argen/mont*	*argentatus*	*G. Himalayan*
397 (6)	P-728	0.373	*argen/mont*	*roylei*	*G. Himalayan*
491 (1)	P-2208	0.415	*argen/mont*	N/A	*G. Himalayan*
491(2)	P-2209	0.437	*argen/mont*	N/A	*G. Himalayan*

TABLE 7.—. External measurements and ratios for *Alticola* from Northern Pakistan. The mean and standard deviations were calculated for available measurements of the five mitochondrial clades. All values except ratios are in mm.

Measurement	**Hindu Kush**	***n***	**Eastern Kohistan**	***n***	**Karakorum**	***n***	**Himalayan**	***n***	**Hushe Valley**	***n***
Head and body	107.9 ± 7.6	15	99.9 ± 10.5	9	101.3 ± 6.9	20	100.9 ± 9.1	43	100.5 ± 6.7	6
Tail	45.6 ± 3.0	15	35.4 ± 2.6	9	46.7 ± 3.7	20	41.8 ± 5.3	43	32.3 ± 2.7	6
Hindfoot	20.7 ± 0.8	15	19.0 ± 0.9	9	20.7 ± 0.8	20	19.9 ± 1.1	44	20.3 ± 0.5	6
Ear	16.5 ± 1.1	15	14.4 ± 1.1	9	16.0 ± 1.0	20	15.0 ± 1.8	44	N/A	0
Tail/Head body	0.424 ± 0.033	15	0.357 ± 0.028	9	0.461 ± 0.032	20	0.416 ± 0.055	43	0.322 ± 0.017	6
Ear/Head body	0.154 ± 0.007	15	0.146 ± 0.014	9	0.158 ± 0.011	20	0.150 ± 0.017	43	N/A	0